Available online at www.sciencedirect.com
SCIENCE DIRECT®
Journal of Nuclear Materials 337–339 (2005) 357–360
journal of nuclear materials
www.elsevier.com/locate/jnucmat

3D Scrape-off layer modelling with BoRiS

J. Riemann *, M. Borchardt, R. Schneider, A. Mutzke

Max-Planck-Institut für Plasmaphysik, Teilinstitut Greifswald EURATOM Association, D-17491 Greifswald, Germany

Abstract

The 3D fluid transport code BoRiS is applied to a hydrogen plasma and a neutral fluid in a stellarator-like geometry equipped with a poloidal ring limiter. The results demonstrate the capability of dealing with 3D effects which can be related to both the influence of the geometry and the plasma–neutral interaction as well. The setup used has similarities with a poloidal gas target in a fusion device.

PACS: 52.25.Ya; 52.55.Dy; 52.55.Hc
Keywords: SOL transport modelling; Edge fluid codes; 3D edge plasma; Neutrals in plasma; Poloidal limiter

1. Introduction

Scrape-off layer (SOL) modelling for fusion plasmas in 3D is of great importance for the understanding of physics as well as for the design of fusion devices. It allows to deal with complex geometries like the new stellarators W7-X and NCSX but also opens a way to study 3D effects in conventional 2D setups, for example a localized gas puff in a tokamak.

BoRiS is a 3D fluid transport code which is motivated by the success of model-validated 2D codes like B2-Eirene and UEDGE [1,2]. It attacks a system of transport equations within a finite volume (FV) approach leading to a coupled system of non-linear partial differential equations which is then linearized and solved with a Newton method utilizing a variety of sophisticated solvers [3]. Complex geometries are taken care of by using magnetic flux (Boozer) coordinates (s, θ, ϕ), which allow standard discretization methods [3] and offer great flexibility. BoRiS has been tested on coupled equations of growing complexity in simplified 1D, 2D and 3D setups [4–6] and is now being applied to a stellarator-like 3D geometry.

2. SOL physics model

The SOL physics model includes continuity equations for both the plasma ($n_a = n_i = n_e$) and the neutral ($n_a = n_0$) densities

$$\frac{\partial}{\partial t}(n_a) + \vec{\nabla}\cdot(n_a \vec{V}_a) = S_n^a, \tag{1}$$

with the velocities according to

$$\vec{V} = \vec{V}_{\parallel,a} + \vec{V}_{\perp,a} = \vec{u}_a + \vec{v}_a. \tag{2}$$

Parallel and perpendicular directions are defined by the traditional (left-handed) curvilinear system $\vec{B}$, $\vec{\nabla}s$, $\vec{\nabla}s \times \vec{B}(\parallel,\perp_1,\perp_2)$.

* Corresponding author.
E-mail address: j.riemann@ipp.mpg.de (J. Riemann).

0022-3115/$ - see front matter
doi:10.1016/j.jnucmat.2004.08.022

Plasma parallel momentum is determined by,

$$\frac{\partial}{\partial t}(m_i n_i u_i) + \vec{\nabla}\cdot(m_i n_i u_i \vec{V}_i - \eta_i \vec{\nabla} u_i) = -\nabla_\parallel p + S^i_{m\parallel}, \quad (3)$$

with viscosity η_i, plasma pressure $p = p_i + p_e$ and a momentum source $S^i_{m\parallel}$ due to interaction with neutrals. Perpendicular flow velocities are obtained from $\vec{v}_i = -D_i \vec{\nabla}_\perp n_i/n_i$ with D_i being an anomalous diffusivity.

In a neutral fluid model with standard assumptions [5], diffusion of neutrals is governed by charge exchange (CX) with $D_0(n_i,T_i) = v^0_{th}/n_i\sigma_{CX}$ and due to the gradient of the neutral gas pressure $p_0 = n_0 T_0$

$$\vec{V}_0 = \vec{u}_0 + \vec{v}_0 = -D_0 \vec{\nabla} p_0/p_0 = -D_0(\vec{\nabla} n_0/n_0 + \vec{\nabla} T_0/T_0), \quad (4)$$

which drives the atoms into the plasma where they are getting ionized and thus contribute to the particle source S^i_n or sink S^0_n in (1).

In the neutral fluid model, CX is dominant and, therefore, ions and neutrals are assumed to form an isothermal ($T_0 = T_i$) heavy ($m_0 = m_i$) species and the internal energy being described by,

$$\frac{\partial}{\partial t}\left(\frac{3}{2}\sum_a p_a\right) + \vec{\nabla}\cdot\left(\frac{5}{2} T_i n_a \vec{V}_a - \sum_a \kappa_a \vec{\nabla} T_i\right) = u_a \nabla_\parallel p_a - Q_{ei} + S^i_q, \quad (5)$$

with conductivities κ_a, heat exchange term Q_{ei} and an ion-neutral heat source S^i_q.

The internal energy equation for the electrons is

$$\frac{\partial}{\partial t}\left(\frac{3}{2} p_e\right) + \vec{\nabla}\cdot\left(\frac{5}{2} T_e n_e \vec{V}_e - \kappa_e \vec{\nabla} T_e\right) = u_e \nabla_\parallel p_e + Q_{ei} + S^e_q, \quad (6)$$

with the electronic conductivities κ_e and the power loss S^e_q. Conductivities and viscosities across the magnetic field are described by isotropic anomalous values to model plasma turbulence while classical expressions are used along magnetic field lines.

3. Geometry setup and boundary conditions

We consider a simplified model of the national compact stellarator experiment (NCSX) originally introduced in [6]. It describes one period of the 3-fold periodic stellarator in terms of magnetic coordinates (s, θ, ϕ), ranging from zero to unity. The model ignores the existence of a perturbed magnetic field outside the last closed magnetic surface (LCMS) and extrapolates closed surfaces instead.

The computational domain is a region between the approximate location of the LCMS at $s = 0.65$ and the wall at $s = 1$ as shown in Fig. 1. In contrast to the actual design of NCSX, we introduced a ring limiter in each module at toroidal position $\phi = 0.5$. This limiter is assumed infinitely thin and cutting into the plasma domain between $0.95 \leqslant s \leqslant 1$. In order to properly resolve the region around the limiter while keeping the mesh comparably small, we use a grid which is non-equidistantly spaced in toroidal direction around $\phi = 0.5$ as well as in the radial direction s. The computational domain is periodically connected in toroidal direction.

The following boundary conditions are used: at the core boundary $s = 0.65$, plasma values are fixed to $T_e = T_i = 50\,\text{eV}$, $n_i = 10^{19}\,\text{m}^{-3}$, $u_i = 0\,\text{m/s}$, and a zero-gradient condition is imposed for the neutrals. At the wall boundary $s = 1$, zero-flux conditions are used for all quantities. At the ring limiter, sheath conditions are set. The recycling of neutrals is set to 0.9 instead of 1.0 (which effectively simulates pumping) and for the charge exchange cross section we assumed $\sigma_{CX} = 10^{-19}\,\text{m}^2$.

4. Results and discussion

The topological properties in the outermost part of the domain are changed by the limiter cutting originally closed field lines. Sheath conditions then accelerate plasma towards the limiter along open field lines. Fig. 2 shows the resulting discontinuity of plasma parallel

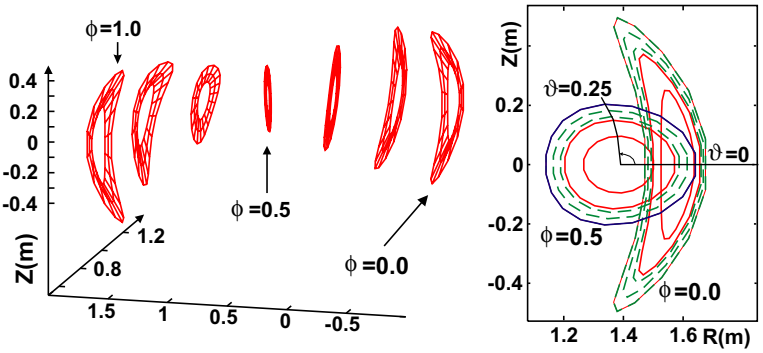

Fig. 1. Cross sections of the NCSX-like module in real space. The insertion shows two sections at $\phi = 0$ and $\phi = 0.5$ with the computational domain (green) for $0.65 \leqslant s \leqslant 1$. The blue ring represents the limiter of radial depth $\Delta s = 0.05$.

velocities $u_i = \pm c_s$ at the limiter. There are only minor variations along the poloidal coordinate θ, being due to almost constant temperatures at the limiter. In the region of closed field lines, u_i develops a quite different pattern as illustrated by Fig. 3. This plot indicates parallel flows with varying $u_i \ll c_s$ along θ and reflects the symmetry of the underlying geometry.

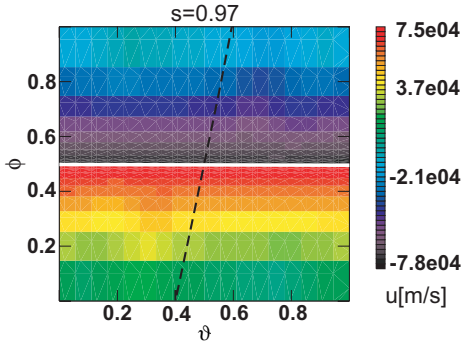

Fig. 2. Plasma parallel velocity u_i on a flux surface $s = 0.97$ (open field lines parallel to dashed line). Velocities reach local sound speeds $\pm c_s$ at the limiter (white line).

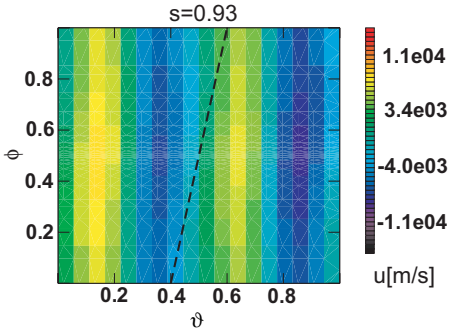

Fig. 3. Plasma parallel velocity $u_i \ll c_s$ on a flux surface $s = 0.93$ (closed field lines parallel to dashed line). The pattern shows a poloidal segmentation with parallel flows in opposite directions.

The plasma flow onto the limiter is partially recycled and forms a source of neutrals which follow the neutral gas pressure gradient back into the domain where they are getting ionized on a spatial scale of the mean free path λ_0. This results in a distribution of neutrals which is clearly peaked in toroidal direction around the limiter position, as shown in Fig. 4. There is a comparably small variation along θ, which reflects the almost constant flow of plasma impinging upon the limiter and thus forming the neutral source. The densities at radial positions

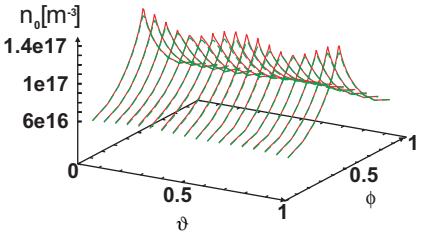

Fig. 4. Neutral density $n_0(\theta, \phi)$ at two radial positions $s = 1$ (red) and $s = 0.65$ (green). The density peaks around the limiter at $\phi = 0.5$.

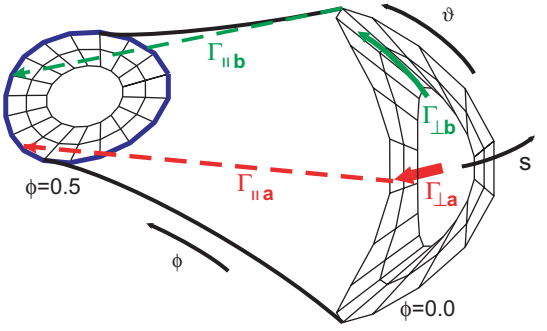

Fig. 6. The computational domain with two cross sections and the system of magnetic coordinates (s, θ, ϕ). Radial fluxes $\Gamma_{\perp a} > \Gamma_{\perp b}$ 'feed' parallel fluxes $\Gamma_{\|a} \approx \Gamma_{\|b}$ of plasma being convected onto the limiter ring.

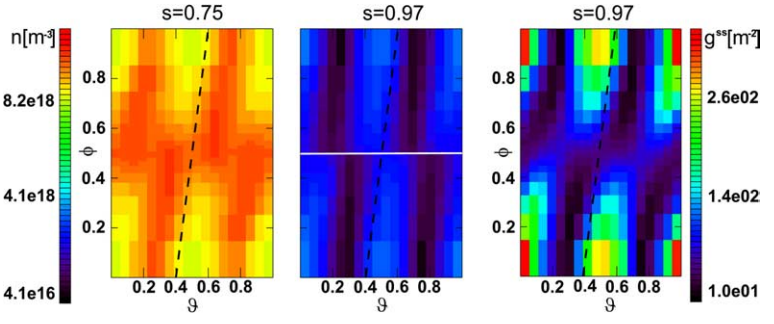

Fig. 5. Plasma density n_i on flux surfaces $s = 0.75$ (left) and $s = 0.97$ (middle) being compared to the metric coefficient g^{ss} (right).

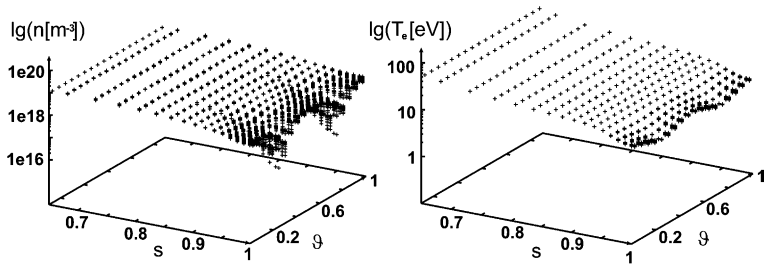

Fig. 7. Plasma density $n_i(s, \theta)$ and electron temperature $T_e(s, \theta)$. The plot actually shows multiple layers corresponding to different ϕ positions.

$s = 0.65$ and $s = 1$ almost appear as a single layer just having a 2D structure in the θ–ϕ plane. This is in agreement with the neutral mean free path λ_0 being large compared to the radial depth ($\approx$0.1 m) of the domain.

The cloud of neutrals around the limiter provides a plasma source where the electron temperature is high enough for ionization to occur, that is in the region of hotter closed field lines ($s < 0.95$), as depicted in Fig. 5. At $s = 0.75$, the density is high around the limiter position with almost no variation along θ. Starting from the limiter, the density pattern mainly follows the magnetic field lines. At $\phi \approx 0$ and $\phi \approx 1$ there is also a clear poloidal modulation of the density which is even more obvious at $s = 0.97$, a surface with open field lines. This profile is related to the underlying metric properties as they are represented by the metric coefficient $g^{ss} = |\vec{\nabla}s|^2$ showing a very similar structure. This quantity can be taken as a measure for the perpendicular particle flux $\Gamma_\perp = -D_i \partial_s n \vec{\nabla}s \cdot \sigma_s \vec{\nabla}s = -D_i \partial_s n g^{ss} \sigma_s$ being driven by a radial density gradient across cell faces $\vec{\sigma}_\perp = \sigma_s \vec{\nabla}s$ with a normal in radial direction. According to Figs. 1 and 6, cell boundaries facing the core at $\theta \approx 0.25$ or $\theta \approx 0.75$ are much smaller than those at $\theta \approx 0$ or $\theta \approx 0.5$. This leads to different radial fluxes $\Gamma_{\perp a} > \Gamma_{\perp b}$ feeding cells with plasma which is then convected along the field with $\Gamma_{\parallel a} \approx \Gamma_{\parallel b}$ due to the pull of the limiter condition. The density profile is thus determined by the different ratios $\Gamma_{\perp a}/\Gamma_{\parallel a} > \Gamma_{\perp b}/\Gamma_{\parallel b}$ as a purely metric effect and is also observed without neutrals.

In Fig. 7, the clear finger print of the metric properties found for the density does not show up for the electron temperature. This is due to the strong parallel electronic heat transport which makes both ratios $\Gamma_{\perp a}/\Gamma_{\parallel a}$ and $\Gamma_{\perp b}/\Gamma_{\parallel b}$ very small anyhow, leading to a radial variation of T_e only.

5. Summary

The BoRiS code was successfully tested on a plasma and neutral fluid model in NCSX-like geometry with a periodic poloidal ring limiter. The result shows 3D effects which can be related to both the geometry and the plasma–neutral interaction. Effects of the topology with closed field lines being cut by the limiter are modulated by the metric properties and result in a 3D structure of the plasma parallel flow. The setup used can serve as a starting point to model a poloidal gas puff forming a neutral gas target in a 3D geometry.

References

[1] R. Schneider et al., Contrib. Plasma Phys. 40 (3&4) (2000) 328.
[2] T.D. Rognlien et al., Contrib. Plasma Phys. 34 (1994) 362.
[3] M. Borchardt et al., in: K. Matsuno, J. Periaux, P. Fox (Eds.), Fluid Dynamics – New Frontiers and Multi-Disciplinary Applications, Elsevier, 2003.
[4] J. Riemann et al., J. Nucl. Mater. 313–316 (2003) 1030.
[5] J. Riemann et al., Contrib. Plasma Phys. 44 (1–3) (2004) 35.
[6] M. Umansky et al., J. Nucl. Mater. 313–316 (2003) 559.